

A SYSTEM TO MONITOR AND MODEL THE THERMAL ISOLATION OF COATING COMPOUNDS APPLIED TO CLOSED SPACES

by

**Frank FLOREZ MONTES^a, Pedro FERNÁNDEZ DE CÓRDOBA^b,
José Luis HIGÓN CALVET^c, J. Alberto CONEJERO^b
and José-Luis POZA-LUJÁN^{d*}**

^a Faculty of Engineering and Architecture, Universidad Nacional de Colombia,
Campus la Nubia, Manizales, Colombia

^b Instituto Universitario de Matemática Pura y Aplicada, Universitat Politècnica de València,
València, Spain

^c Department of Architectural Graphic Expression, Universitat Politècnica de València,
València, Spain

^d Instituto Universitario de Automática e Informática Industrial, Universitat Politècnica de València,
Valencia, Spain

Original scientific paper
<https://doi.org/10.2298/TSC190525077M>

Smart control systems and new technologies are necessary to reduce the energy consumption in buildings while achieving thermal comfort. In this work, we monitor the thermal evolution inside a scale reduced closed space whose exterior and/or interior wall faces have been painted with a coating solution. Based on the experimental data obtained under different environmental conditions, a simulator was developed and tuned to reproduce the thermodynamic behavior inside the spaces, with a relative error of less than 3.5%. This simulator lets us also estimate energy savings, temperature, and flux behavior under other conditions.

Key words: coating, thermal isolation, building modeling, energy savings

Introduction

The reduction of energy consumption is a critical factor for urban sustainability. The main efforts are associated with achieving thermal comfort in residential and commercial buildings [1, 2]. Different technologies and strategies are alternatives to the use of HVAC systems, which have been historically criticized for their high energy consumptions.

Passive strategies search to mitigate the heat transfer between the thermal zones and the environment, using new materials and alloys for construction or retrofitting in order to give buildings a better resistance against the environmental conditions [3]. However, these solutions are still in development and its deployment is subject to the economic cost, durability, climatic factors, and facilities of installation.

Passive techniques for thermal isolation can be classified according to different aspects, such as the heat exchange properties, composition, and form [4]. Additionally, depending on its use of shading or isolation, it can incorporate ambient benefits. For example, the installation of photovoltaic panels on the rooftop of a building permits to generate electric energy in

* Corresponding author, e-mail: jopolu@upv.es

situ and to approximate the building to a zero consume [5, 6]. Another important initiative is the use of the green roofs that change the surfaces albedo and reduce the solar radiation absorption. Besides, they also report ambient benefits such as the stormwater retention, the reduction of the urban heat island effect, and the increase of the roofs lifespan [7].

Retrofitting of existing buildings and reducing the use of HVAC systems, is a trending line of research around the world [8, 9]. The effect of materials such as aerogels, cork lime and PIR over the thermal transmittance of the walls of a historic building in Dublin was analyzed in [10]. In India, the isolation given by a thermal paint on the facade and rooftop of a building provided reductions of 4.4 °C [11]. Similarly, in Shanghai, the reflectance of the walls after applying thermal paints increase from 32% until 61% [3].

Most of these passive strategies are designed and tested in warm regions, since they present problems of holding back the heat contained in buildings on cold regions. Nevertheless, coating solutions can be adjusted for both climates. They consist on their application over the faces of the building to be thermally isolated. On the one hand, if they are applied on the interior surfaces, they can create a greenhouse effect reducing the warming needs of the people living there. On the other hand, their application on the external surfaces can increase the convection process to evacuate the internal heat or to reflect the solar radiation [12-14].

To quantify thermal reductions and energy savings of thermal coating solutions, experimental results are needed. They can be obtained from existing buildings, from experiments on a lab, where environmental conditions are controlled [2, 15], or from a combination of both of them. In any case, the development of a mathematical model would permit to extrapolate the results to different conditions.

In this article, we construct and validate such a model to quantify the thermal isolation and energy savings of a coating solution with low thermal conductivity. More information on the thermal conductivity properties of polymers at molecular level can be found in [16].

We built three scale-reduced models. They were evaluated indoor, for minimizing the effect of environmental disturbances, and outdoor, for evaluating the influence of the weather conditions. We designed a control system to collect data from the experiments. Based on the experimental data recorded, we developed a simulator that can reproduce the obtained experimental results with high accuracy. It allows us to estimate the behavior of the models under different experimental conditions.

Design of the experiments and methodology

We have considered a water-proof insulating coating with very low thermal conductivity and high resistance to weathering. It has a stable aqueous dispersion and is formed of a very heavy molecular styrene-acrylic polymer. The product presents a thermal conductivity $\lambda = 0.0556$ W/mK.

To test the effect of this coating solution on heat transfer, we built three reduced scale thermal zones with wooden boxes (named *U*, *I*, *O*) of dimensions $0.4 \times 0.545 \times 0.7$ m³ and thickness of 15.8 mm. Each box is equipped with a 60 W incandescent internal lamp with infrared light to generate thermal gradients between the air contained in the box and the air outside. Box *U* was left in its original state (unpainted), with no coating applied on their surfaces. We apply a coating layer of 0.5 mm on the inner faces of box *I*. Finally, a similar coating layer was applied on the outer surfaces of box *O*. In each one of the boxes, an electrical installation was implemented in order to supply energy to the internal lamp and to the temperature and humidity sensor Data Logger Wholer CDL. The final result is shown in fig. 1. To guarantee the correct development of the experiment, and to reduce sources of interruption, we initially

carried out tests of ignition cycles with the models in a closed space, where abrupt changes in ambient temperature and solar radiation were minimized.

To manage the experiments, we developed a distributed control system that allowed varying temperatures, validating conditions, and managing data collection. Each box has a control node, based on Arduino, that allows it to change temperature, to validate the conditions, and to manage the data collected. Control nodes are connected to a database server in order to get experiments configuration and to send the data collected. This system allows planning cycles of experiments for each box. With this, we can contrast the data collected by the sensors with the conditions in order to ensure the coherence of the results.



Figure 1. Wooden boxes *U*, *I*, and *O* with internal gains

Mathematical model and tuning process

We have considered a simulator based on the mathematical model, obtained with the technique of Lumped Parameters, which is described in [17]. This model lays on the analogy between thermal and electrical phenomena. More precisely, the temperature is represented by voltage, the heat flux by an electric current, thermal resistance is defined as the resistance to heat transfer through walls, and the wall's capacity to accumulate energy is identified with capacitors. The following equations described the transfer processes in any one of the boxes, whose six faces are indexed with $i = 1, \dots, 6$:

$$\frac{dT_{i,ex}}{dt} = \frac{T_i}{R_{i,ex}C_{i,ex}} - T_{i,ex} \left(\frac{1}{R_{i,ex}C_{i,ex}} + \frac{1}{R_{i,mid}C_{i,ex}} \right) + \frac{T_{i,in}}{R_{i,mid}C_{i,ex}} \quad (1)$$

$$\frac{dT_{i,in}}{dt} = \frac{T_{i,ex}}{R_{i,mid}C_{i,in}} - T_{i,in} \left(\frac{1}{R_{i,mid}C_{i,in}} + \frac{1}{R_{i,in}C_{i,in}} \right) + \frac{T}{R_{i,in}C_{i,in}} \quad (2)$$

$$\frac{dT}{dt} = \frac{T_{1,in} - T}{R_{1,in}C_r} + \frac{T_{2,in} - T}{R_{2,in}C_r} + \frac{T_{3,in} - T}{R_{3,in}C_r} + \frac{T_{4,in} - T}{R_{4,in}C_r} + \frac{T_{5,in} - T}{R_{5,in}C_r} + \frac{T_{6,in} - T}{R_{6,in}C_r} + \frac{uI_L}{C_r} \quad (3)$$

The internal heat source is represented by uI_L , where I_L is the heat power source, and u is the source state. $T_{i,in}$ and $T_{i,ex}$ are superficial temperatures, and the internal temperature is presented by T . Capacitors C_r , $C_{i,in}$ and $C_{i,ex}$, and resistors $R_{i,mid}$ are calculated in terms of the physical parameters of the materials (wood and internal air) summarized in tab. 1. Resistances $R_{i,in}$ and $R_{i,ex}$ are calculated with the convection and radiation coefficients that are tuned to the specific conditions of the test. For convection with natural ventilation we initially took 60 kJ and the emissivity coefficient of white painted wood was set to 0.9, [17, 18]. With these values, we run a fitting algorithm to look for the values of the parameters that provide a best fitting of the solutions respect to the data obtained from the indoor experiments. Later, these values let us calculate the resistances and capacitors in eqs. (1)-(3). Results are presented in tab. 2.

Table 1. Coating solution and material parameters

Material	Parameter	Value
Wood	Conductivity	0.645 kJ/hmK
	Density	700 kg/m ³
	Specific heat	1.6 kJ/kgK
Air	Density	1.2 kg/m ³
	Specific heat	1.007 kJ/kgK
Coating solution	Density	1250 kg/m ³
	Conductivity	0.2002 kJ/hmK

Indoor simulation and experimental results

A first indoor test was required to tune the convection and radiation coefficients of the internal and external surfaces of the boxes. That experiment was conducted on March 15th, 2018, and it lasted 24 hours. The first 6 hours the lamp was turned on, producing a period of charge and heat transfer from the air contained in the boxes to the environment, which remained in the range of 14.6 °C to 17.3 °C, with an average temperature of 16 °C. For the rest of the test, the lamp was off. With these experimental

data, we determined the best values for tuning the heat transfer coefficients for each box and lamp state, see tab. 2, by using the Pattern Search optimization algorithm of Matlab OptimTool. Here, h_i and h_o are the internal and external convection coefficients, and e_i and e_o are the internal and external emissivity of the surfaces.

Table 2. Heat transfer coefficients

Box	Lamp state	h_i [kJh ⁻¹ m ⁻² K ⁻¹]	h_o [kJh ⁻¹ m ⁻² K ⁻¹]	e_i	e_o
U (unpainted)	Active	44.6875	11.1250	0.9430	0.9
	Inactive	0	9.7324	0.0211	0.8805
O (outer)	Active	44.6875	19.0938	0.9430	0.9
	Inactive	0	10.4910	0.0211	0.8
I (Inner)	Active	20.4805	11.1250	0.99	0.9
	Inactive	0.2578	9.7324	0.0190	0.8805

Comparing the real temperatures with the ones provided by the simulations, see fig. 2, we obtain an error of around 3% (2.7% in box *U*, 2.8% in box *I*, and 3.5% in box *O*). It is possible that replacing derivatives by fractional derivatives would improve the predictions, see [19].

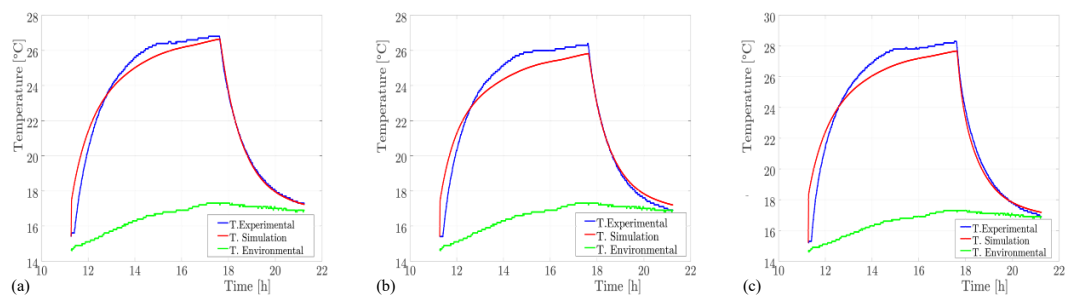


Figure 2. Temperatures during the indoor experiment at boxes *U* (a), *I* (b), and *O* (c)
(for color image see journal web site)

Simulation and experimental results outdoors

On July 12th, 2018, we conducted an outdoor experiment in a protected space. As in the indoor experiment, the tests were carried out with the same data logger. Additionally, contact sensors (DS18B20) were used to measure the surface temperatures of the upper and lower faces in each box. The central data acquisition was done with an ESP32 LOLIN32 Lite

card. Initially, continuous loading and unloading tests were carried out, beginning at 12:00 p. m. The loading phases lasted 8 hours, while discharge phases lasted only 4 hours. Figure 3 shows the evolution of the internal temperature in all the boxes along three days of sampling.

As previously mentioned, internal and external surface temperatures were also measured. Figure 4 shows the evolution of these temperatures at each box. With these data, it is possible to calculate the thermal transmittance T defined by eq. (4), where L and k define the thickness and conductivity of the walls [20]:

$$T = \frac{1}{\frac{1}{h_i} + \frac{1}{h_o} + \frac{L}{k}} \quad (4)$$

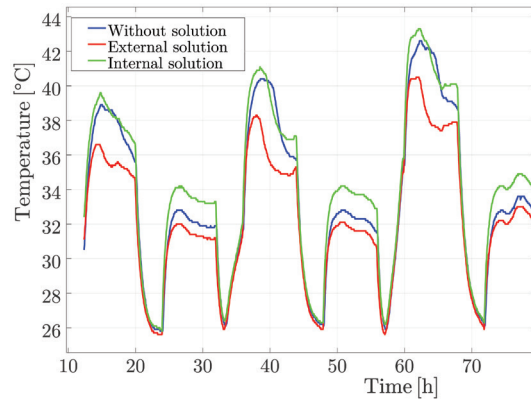


Figure 3. Experimental results in all the boxes during outdoor experiments (for color image see journal web site)

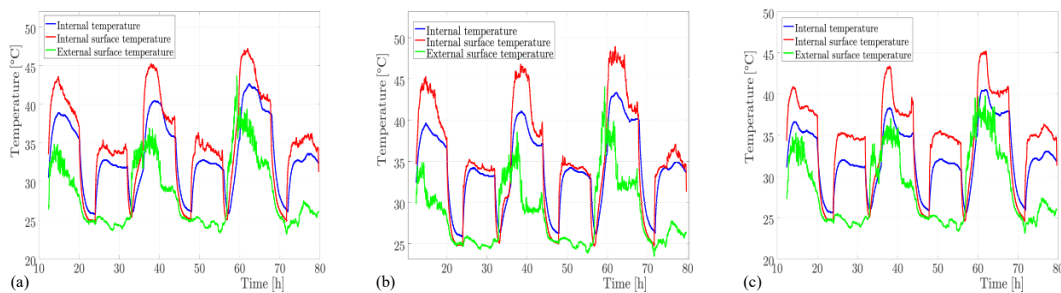


Figure 4. Internal and superficial temperature of box U (a), I (b), and O (c) (for color image see journal web site)

During the active periods of the day, the transmittance values at the boxes were: 6.1124 kJ/hm²K at box U , 7.2939 kJ/hm²K at box I , and 1.004 kJ/hm²K at box O . With these results, we conclude that for high external temperatures, it is counterproductive to paint the internal faces of the boxes.

The next test was performed on July 19th, 2018. This time the lamp was turned off during the entire test. The average environmental temperature was 35 °C. Figure 5 shows the temperature registered inside boxes U and O , since it lacks of sense to study box I in this case.

In order to properly reproduce the outdoor data, it was also necessary to adjust the model to the new environmental conditions. One of the main differences between both situations is the ambient radiation: in the case of the indoor tests it was practically constant while in the open air it changes considerably throughout the day. The interaction of a body with the environment by radiation is defined by the Stefan-Boltzman law showed in eq. (5). This allows to calculate the heat absorbed and issued from and to the environment by any surface. The radiation emission coefficient, ε , depends on the material, while the absorption coefficient, α , is

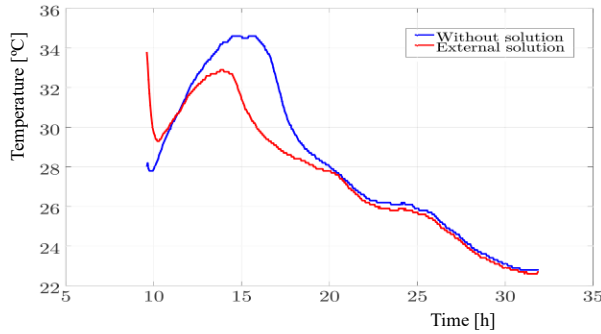


Figure 5. Internal temperature of boxes *U* and *O* during outdoor experiments (for color image see journal web site)

related to the ambient radiation [21]. The surface and environmental temperatures are denoted by T_{surf} and T_{env} and Q stands for the heat transferred by radiation:

$$\dot{Q} = \epsilon\sigma T_{surf}^4 - \alpha\sigma T_{env}^4 \quad (5)$$

Another important treatment of the simulation was the establishment of three periods of analysis. We show in tab. 3 the coefficients for each period. Figure 6(a) shows the results obtained from the simulator for box *U*, with an error of 1.6% with respect to the experimental data, while fig. 6(b) shows the results for box *O*, with an error of 2.2%.

Table 3. Parameters adjusted to outdoor environmental conditions.

Box	Time	h_i [kJh ⁻¹ m ⁻² K ⁻¹]	h_o [kJh ⁻¹ m ⁻² K ⁻¹]	ϵ	α
Unpainted	8:00-12:00	0.1777	7.9688	0.9992	0.9323
	12:00-20:00	0.0542	22.48	0.9992	0.9323
	20:00-24:00	0.0542	22.48	0.9992	0.9870
External faces painted	8:00-12:00	68.4836	0.9332	0.9992	0.91
	12:00-20:00	0.0107	0.0254	0.9992	0.8591
	20:00-24:00	0.1	4.6666	0.9992	0.9705

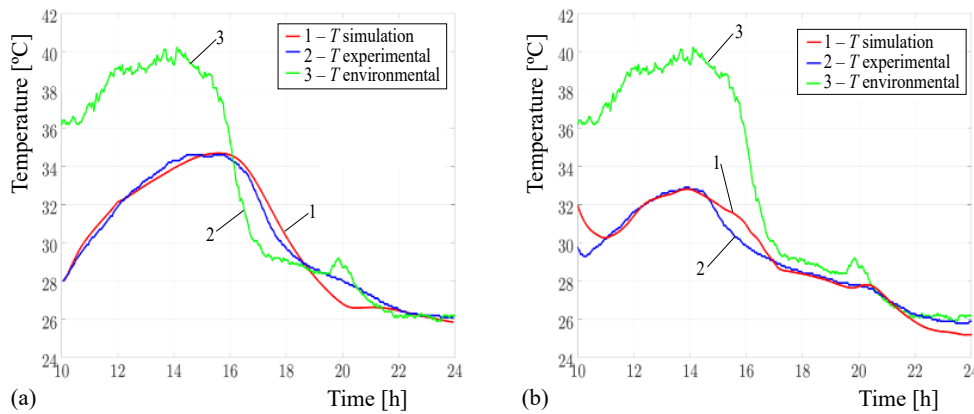


Figure 6. Experimental and simulated results on boxes *U* (a) and *O* (b) (for color image see journal web site)

Energy savings

Quantify energy savings is a hard task, since it depends on different factors such as electric sources, collection fees in each country, and seasonal factors [22]. However, temperature reductions are directly proportional to energy savings. We have determined the savings by comparison of the temperature in boxes with coating, *I* and *O*, respect to the unpainted one, *U*.

With an average environmental temperature of 16 °C, the energy savings obtained by taking box *I* instead of box *U* are of around a 4.5%, and with an environmental temperature of 35 °C, the energy savings obtained when taking *O* instead of *U* are around 7.4%.

Finally, we have used our simulator for estimating energy savings on larger spaces and with different external temperatures. The original experiment had a volume of $v_1 = 0.153 \text{ m}^3$ and we used an internal lamp of 60 W. For these new estimations, we have considered two different volumes: $v_2 = 14.98 \text{ m}^3$ and $v_3 = 47.3 \text{ m}^3$; the last volume corresponds to a maritime container and the second one is an intermediate value. Setting the maritime container in a place with an external temperature of 35 °C (or the intermediate volume in a place with external temperature of 30 °C), the energy savings move up to 15%.

Conclusions

During the project development, reduced scale models were used to verify the impact of applying a coating solution to the internal and external faces of a building. The experiments were carried out using a distributed control system. That allows to configure a large number of possible experiments. Consequently, it is possible to collect data with adequate conditions to design the simulation. The indoor and outdoor tests allowed us to design an accurate simulator to analyze and reproduce the experimental results. This also let us predict energy savings with different models and under environmental conditions, and the determine the convenience of using a coating solution.

First, we conclude that a greenhouse effect is generated when painting the internal faces of a closed space, since this prevents the heat flow from internal sources to the environment, which would be of interest for cold climates, where the efforts must be pointed to preserve the thermal energy in the interior of the thermal zones. Secondly, applying the solution on the outer faces contributes to significantly reduce the inner temperature, which would be interesting for warm climates.

For future work we leave the evaluation of coatings on different models with materials such as concrete and metal. Besides, it can be of interest to evaluate the effectiveness of the solution in locations with environmental temperatures under 0 °C.

Acknowledgment

This research was supported by the National Doctoral Program of the Colombian Administrative Department of Science Technology and Innovation (Colciencias).

References

- [1] Pan, L., et al., Analysis of Climate Adaptive Energy-Saving Technology Approaches to Residential Building Envelope in Shanghai, *J. Build. Eng.*, 19 (2018), Sept., pp. 266-272
- [2] Yew, M. C., et al., Experimental Analysis on the Active and Passive Cool Roof Systems for Industrial Buildings in Malaysia, *J. Build. Eng.*, 19 (2018), Sept., pp. 134-141
- [3] Moradias, P., et al., Experimental Study on Hygrothermal Behaviour of Retrofit Solutions Applied to Old Building Walls, *Constr. Build. Mater.*, 35 (2012), Oct., pp. 864-873
- [4] Aditya, L., et al., A Review on Insulation Materials for Energy Conservation in Buildings, *Renew. Sust. Eng. Rev.*, 73 (2017), June, pp. 1352-1365
- [5] Kapsalis, V., Karamanis, D., On the Effect of Roof Added Photovoltaics on Building's Energy Demand, *Energy Build.*, 108 (2015), Dec., pp. 195-204
- [6] You, S., et al., On the Temporal Modelling of Solar Photovoltaic Soiling: Energy and Economic Impacts in Seven Cities, *Appl. Energy*, 228 (2018), Oct., pp. 1136-1146
- [7] Scherba, A., et al., Modeling Impacts of Roof Reflectivity, Integrated Photovoltaic Panels and Green Roof Systems on Sensible Heat Flux into the Urban Environment, *Build. Environ.*, 46 (2011), 12, pp. 2542-2551

- [8] Pisello, A. L., State of the Art on the Development of Cool Coatings for Buildings and Cities, *Sol. Energy*, 144 (2017), Mar, pp. 660-680
- [9] Hernandez-Perez, I., *et al.*, Thermal Performance of Reflective Materials Applied to Exterior Building Components – A Review, *Energy Build.*, 80 (2014), Sept., pp. 81-105
- [10] Walker, R., Pavia, S., Thermal Performance of a Selection of Insulation Materials Suitable for Historic Buildings, *Build. Environ.*, 94 (2015), 1, pp. 155-165
- [11] Jain, M., Pathak, K., Thermal Modelling of Insulator for Energy Saving in Existing Residential Building, *J. Build. Eng.*, 19 (2018), Sept., pp. 62-68
- [12] Becherini, F., *et al.*, Characterization and Thermal Performance Evaluation of Infrared Reflective Coatings Compatible with Historic Buildings, *Build. Environ.*, 134 (2018), Apr., pp. 35-46
- [13] Fantucci, S., Serra, V., Investigating the Performance of Reflective Insulation and Low Emissivity Paints for the Energy Retrofit of Roof Attics, *Energy and Buildings*, 182 (2019), Jan., pp. 300-310
- [14] Azemati, A. A., *et al.*, Thermal Modeling of Mineral Insulator in Paints for Energy Saving, *Energy Build.*, 56 (2013), Jan., pp. 109-114
- [15] Shafiq, P., *et al.*, Concrete as a Thermal Mass Material for Building Applications - A Review, *J. Build. Eng.*, 19 (2018), Sept., pp. 14-25
- [16] Huang, C., *et al.*, Thermal Conductivity of Polymers and Polymer Nanocomposites, *Materials Science and Engineering: R: Reports*, 132 (2018), pp. 1-22
- [17] Florez, F., *et al.*, Modeling, Simulation, and Temperature Control of a Thermal Zone with Sliding Modes Strategy, *Mathematics*, 7 (2019), 6, 503
- [18] Cengel, Y., *Transferencia De Calor Y Masa*, McGraw Hill, New York, USA, 2007
- [19] Brzezinski, D., Review of Numerical Methods for NumILPT with Computational Accuracy Assessment for Fractional Calculus, *Applied Mathematics Nonlinear Sciences*, 3 (2018), 2, pp. 1487-1502
- [20] Lienhard IV, J. H., Lienhard V, J. H., *A Heat Transfer Textbook*, 3rd ed., Phlogiston Press, Cambridge, Mass., USA, 2001
- [21] Incropera, F. P., *et al.*, *Fundamentals of Heat and Mass Transfer*, John Wiley and Sons, 6th ed., New York, USA, 2007
- [22] Ruiz-Fernandez, J. P., *et al.*, Influence of Seasonal Factors in the Earned Value of Construction, *Applied Mathematics Nonlinear Sciences*, 4 (2019), 1, pp. 21-34